



# Fully developed mixed convection and flow reversal in a vertical rectangular duct with uniform wall heat flux

A. Barletta \*

*Dipartimento di Ingegneria Energetica, Nucleare e del Controllo Ambientale (DIENCA), Università di Bologna,  
Viale Risorgimento 2, I-40136 Bologna, Italy*

Received 10 January 2001; received in revised form 30 March 2001

## Abstract

Combined forced and free flow in a vertical rectangular duct is investigated for laminar and fully developed regime. The velocity field, the temperature field, the friction factor and the Nusselt number are evaluated analytically by employing finite Fourier transforms. The thermal boundary condition considered is an axially uniform wall heat flux and a peripherally uniform wall temperature, i.e. an H1 boundary condition. The necessary and sufficient condition for the onset of flow reversal is determined either in the case of upward flow in a cooled duct or in the case of downward flow in a heated duct. The special case of free convection, i.e. the case of a purely buoyancy-driven flow, is discussed. The occurrence of effects of pre-heating or pre-cooling in the fluid is analysed. It is pointed out that although these effects occur in rectangular ducts, they are not present either in circular ducts or in parallel-plate channels. © 2001 Elsevier Science Ltd. All rights reserved.

*Keywords:* Laminar flow; Mixed convection; Rectangular duct; Analytical methods

## 1. Introduction

In a recent paper [1], an investigation of fully developed mixed convection in a vertical rectangular duct is presented. In this paper, an analytical solution of the energy and momentum balance equations is obtained, by employing the finite Fourier transform method. The solution refers to a class of thermal boundary conditions such that at least one of the four walls of the rectangular duct is kept isothermal. Thermal boundary conditions in this class imply the axial invariance of the temperature distribution in the fully developed region. Obviously, there are thermal boundary conditions of interest in engineering applications which are not included in the above-defined class. For instance, a thermal boundary condition often invoked in duct-flow heat transfer is the H1 boundary condition. As is well known, the H1 boundary condition corresponds to an axially uniform

wall heat flux and a peripherally uniform wall temperature. Obviously, under this boundary condition, no axial invariance of the temperature distribution in the fully developed region occurs, so that the H1 case does not belong to the class investigated in [1]. An extension of the analysis presented in [1] to include the H1 boundary condition is the purpose of the present paper.

As is well known, heat exchangers technology, the design of solar collectors or the modelling of cooling processes in electronic devices involve convective flows in non-circular ducts. In most cases, these applications imply conditions of uniform heating of a duct which can be modelled either by the H1 boundary condition or by the H2 boundary condition. The latter case corresponds to a wall heat flux both axially and peripherally uniform. The subject of forced and mixed convection in rectangular ducts with uniform heating conditions has been widely treated in the literature. An accurate review on this subject can be found in [2]. Among the earlier investigations in this field, the paper by Han [3] presents an analytical solution for combined forced and free flow in a vertical rectangular duct, which refers to the fully developed region and to an H1 boundary condition.

\* Tel.: +39-51-209-3295; fax: +39-51-209-3296.

E-mail address: antonio.barletta@mail.ing.unibo.it (A. Barletta).

| Nomenclature |   |                                  |  |
|--------------|---|----------------------------------|--|
| $a, b$       | length of the rectangle sides   | $Re$                             | Reynolds number, defined in Eq. (15)                     |
| $C_{n,m}$    | dimensionless coefficients defined by Eq. (36)                                | $t$                              | dimensionless temperature, defined in Eq. (15)           |
| $D$          | $= 2ab/(a + b)$ , hydraulic diameter  | $T$                              | temperature  |
| $f$          | Fanning friction factor, defined in Eq. (23)                                  | $T_0$                            | mean temperature in a duct section                       |
| $F_1$        | dimensionless quantity defined by Eq. (41)                                    | $T_w$                            | wall temperature   |
| $F_2$        | dimensionless quantity defined by Eq. (42)                                    | $u$                              | dimensionless velocity, defined in Eq. (15)              |
| $g$          | magnitude of the gravitational acceleration                                   | $U$                              | Z-component of the fluid velocity                        |
| $Gr$         | Grashof number, defined in Eq. (15)   | $U_0$                            | mean fluid velocity in a duct section                    |
| $(Gr/Re)'$   | threshold value of $Gr/Re$ for the onset of flow reversal                     | $W(x, y)$                        | arbitrary function                                       |
| $(Gr/Re)''$  | value of $Gr/Re$ corresponding to free convection                             | $x, y$                           | dimensionless coordinates, defined in Eq. (15)           |
| $(Gr/Re)'''$ | value of $Gr/Re$ corresponding to the first singularity of the solution       | $X, Y, Z$                        | rectangular coordinates                                  |
| $(Gr/Re)_t$  | threshold value of $Gr/Re$ for the onset of pre-heating (pre-cooling) effects | <i>Greek symbols</i>             |  |
| $k$          | thermal conductivity  | $\alpha$                         | thermal diffusivity                                      |
| $n, m$       | positive integers   | $\beta$                          | volumetric coefficient of thermal expansion              |
| $Nu$         | Nusselt number defined by Eq. (25)  | $\Delta T$                       | $= \bar{q}_w D/k$ , reference temperature difference     |
| $Nu_0$       | $T_0$ -based Nusselt number defined by Eq. (27)                               | $\lambda$                        | dimensionless parameter defined by Eq. (15)              |
| $p$          | pressure  | $\eta$                           | dimensionless parameter defined by Eq. (15)              |
| $P$          | difference between the pressure and the hydrostatic pressure                  | $\mu$                            | dynamic viscosity  |
| $\bar{q}_w$  | average wall heat flux  | $\nu$                            | kinematic viscosity                                      |
| $R(x, y)$    | arbitrary function  | $\rho$                           | mass density   |
|              |   | $\rho_0$                         | mass density for $T = T_0$                               |
|              |   | $\sigma$                         | $= b/a$ , aspect ratio                                   |
|              |   | $\tau_{w,m}$                     | average wall shear stress                                |
|              |   | <i>Superscript and subscript</i> |  |
|              |   | $\approx$                        | double finite Fourier sine transform defined by Eq. (28) |
|              |   | $b$                              | bulk value   |

However, the analysis presented in [3] is not complete, since no discussion of the phenomenon of flow reversal is performed. As is well known, flow reversal occurs in a given duct section if there exist positions where the local fluid velocity has a direction opposite to the mean flow. Moreover, the mathematical model of mixed convection employed in [3] is not completely satisfactory as is pointed out in Section 4 of the present paper.

More recently, investigations on mixed convection in vertical rectangular ducts or parallel-plate channels have appeared in the literature, involving in most cases the use of numerical or experimental methods. Ingham et al. [4] employ a fully implicit finite difference scheme to obtain a solution for the velocity and temperature field in the entrance region of a vertical parallel-plate channel with uniform and unequal wall temperatures. Gau et al. [5] provide an experimental investigation of the phenomenon of flow reversal in a vertical channel, by employing flow visualization in a wind tunnel. Cheng

et al. [6] obtain a numerical solution of the mass, momentum and energy balance equations in the entrance region of a vertical rectangular duct such that one wall is maintained at a higher temperature and the other three walls are kept isothermal at a lower temperature. These authors employ an enhanced FLARE method in order to encompass also situations involving flow reversal. A wide analysis of various modifications of the FLARE method for two-dimensional mixed convection in a vertical parallel-plate channel including flow reversal is performed by Cheng et al. [7]. Lee [8] utilizes the vorticity-velocity formulation to obtain a numerical solution of the balance equations for buoyancy-induced heat and mass transfer in a vertical rectangular duct. This author assumes that three duct walls are adiabatic, while the fourth is kept at a uniform temperature or at a uniform heat flux. By employing analytical methods, McBain [9] performs an investigation of buoyancy-induced flow and mass transfer in the fully developed

region of a vertical rectangular duct with two isothermal walls and two adiabatic walls. The numerical study presented in [6] has been recently extended to consider mixed convection in a vertical rectangular duct such that one or more walls are kept isothermal at a higher temperature while the others are isothermal at a lower ambient temperature [10].

The aim of the present paper is to study mixed convection heat transfer in a vertical rectangular duct subjected to an H1 thermal boundary condition. The analysis refers to the region of fully developed flow where the velocity field is parallel. An analytical method involving finite Fourier transforms is employed to yield the solution of the coupled momentum and energy balance equations. For the cases of either upward flow in a cooled duct or of downward flow in a heated duct, the necessary and sufficient condition for the onset of flow reversal is obtained. A novel feature of fully developed mixed convection in vertical ducts which does not occur either in parallel-plate channels or in circular ducts is described. In particular, it is shown that a sufficiently intense flow reversal in a vertical rectangular duct may yield a pre-heating or pre-cooling of the fluid. In other words, even if the walls are heated, there may exist positions in a given duct section where the local temperature is higher than the wall temperature. A description of this effect and a statement of the necessary and sufficient condition for its onset are given in Section 5 of this paper.

## 2. Governing equations

The system under analysis is a Newtonian fluid flowing in an infinitely long vertical duct with a rectangular cross-section. A drawing of the system examined and of the coordinate axes is reported in Fig. 1. The

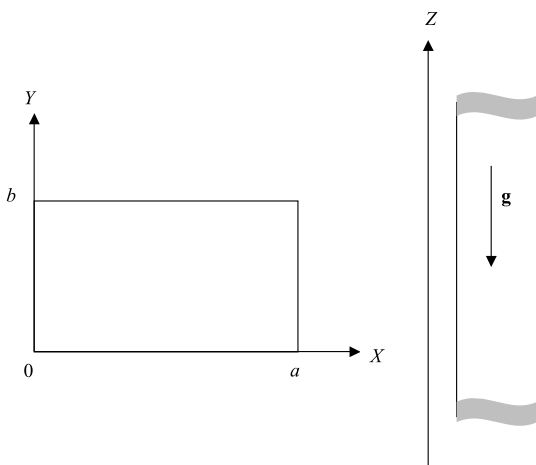


Fig. 1. Drawing of the duct and of the coordinate axes.

flow is assumed to be steady, laminar and parallel, i.e. only the Z-component  $U$  of the fluid velocity  $\mathbf{U}$  is non-vanishing. The thermal conductivity  $k$ , the thermal diffusivity  $\alpha$  and the dynamic viscosity  $\mu$  are considered as constant. Moreover, the effect of viscous dissipation is neglected and the Boussinesq approximation is employed. Since the Boussinesq approximation implies that the velocity field is solenoidal, i.e. that  $\partial U / \partial Z = 0$ , one can conclude that  $U$  does not depend on  $Z$ . Therefore, the X-momentum balance equation, the Y-momentum balance equation, the Z-momentum balance equation and the energy balance equation for the fluid can be written as

$$\frac{\partial P}{\partial X} = 0, \quad \frac{\partial P}{\partial Y} = 0, \quad (1)$$

$$\rho_0 g \beta (T - T_0) - \frac{\partial P}{\partial Z} + \mu \left( \frac{\partial^2 U}{\partial X^2} + \frac{\partial^2 U}{\partial Y^2} \right) = 0, \quad (2)$$

$$U \frac{\partial T}{\partial Z} = \alpha \left( \frac{\partial^2 T}{\partial X^2} + \frac{\partial^2 T}{\partial Y^2} + \frac{\partial^2 T}{\partial Z^2} \right). \quad (3)$$

The scalar field  $P = p + \rho_0 g Z$  is the difference between the pressure and the hydrostatic pressure and  $T_0$  is a reference temperature which should ensure that the linear relation between the local mass density and the local temperature

$$\rho = \rho_0 [1 - \beta (T - T_0)] \quad (4)$$

is a fair approximation. Whenever the reference temperature  $T_0$  changes in the streamwise direction, the Boussinesq approximation can still be employed provided that the dependence of  $\rho_0$  on  $Z$  is neglected. This assumption [11,12] is widely employed in the literature if the thermal boundary conditions imply a net heating or cooling of the fluid. In [13], it is shown that the optimal choice of  $T_0$  in order to fulfil Eq. (4) is the mean temperature in a duct section, namely

$$T_0 = \frac{1}{ab} \int_0^a dX \int_0^b dY T. \quad (5)$$

On account of Eq. (1),  $P$  is independent of both  $X$  and  $Y$ . If Eq. (2) is derived with respect to  $Z$ , one obtains

$$\frac{\partial T}{\partial Z} = \frac{dT_0}{dZ} + \frac{1}{\rho_0 g \beta} \frac{d^2 P}{dZ^2}. \quad (6)$$

As a consequence of Eq. (5), by performing a double integration of both sides of Eq. (6) with respect to  $X$  and  $Y$  in the domain  $\{0 \leq X \leq a, 0 \leq Y \leq b\}$ , one is led to the following conclusions:  $dP/dZ$  is a constant;  $\partial T / \partial Z$  coincides with  $dT_0 / dZ$ .

The local energy balance given by Eq. (3) can be rewritten as

$$U \frac{dT_0}{dZ} = \alpha \left( \frac{\partial^2 T}{\partial X^2} + \frac{\partial^2 T}{\partial Y^2} + \frac{d^2 T_0}{dZ^2} \right). \quad (7)$$

The rate of change  $dT_0/dZ$  can be determined when the thermal boundary conditions are given.

Let us assume that an axially uniform heat flux is prescribed on the duct wall and that the wall temperature is peripherally uniform, i.e. that an H1 boundary condition holds. Then, while the wall temperature  $T_w$  depends only on  $Z$  and is a priori unknown, the peripherally averaged wall heat flux  $\bar{q}_w$  is a prescribed constant which can be expressed as

$$\bar{q}_w = \frac{k}{2(a+b)} \left[ \int_0^b \left( \frac{\partial T}{\partial X} \Big|_{X=a} - \frac{\partial T}{\partial X} \Big|_{X=0} \right) dY + \int_0^a \left( \frac{\partial T}{\partial Y} \Big|_{Y=b} - \frac{\partial T}{\partial Y} \Big|_{Y=0} \right) dX \right]. \quad (8)$$

By employing Eqs. (5) and (8), a double integration of Eq. (7) with respect to  $X$  and  $Y$  in the domain  $\{0 \leq X \leq a, 0 \leq Y \leq b\}$  yields

$$U_0 \frac{dT_0}{dZ} - \alpha \frac{d^2 T_0}{dZ^2} = \frac{4\alpha \bar{q}_w}{kD}, \quad (9)$$

where  $D = 2ab/(a+b)$  is the hydraulic diameter and  $U_0$  is the mean velocity given by

$$U_0 = \frac{1}{ab} \int_0^a dX \int_0^b dY U. \quad (10)$$

Since  $\partial T/\partial Z$  coincides with  $dT_0/dZ$ , one can conclude that  $\partial T/\partial Z$  depends neither on  $X$  nor on  $Y$ . Then, if one evaluates the derivative with respect to  $Z$  of both sides of Eq. (7), one obtains

$$U \frac{d^2 T_0}{dZ^2} - \alpha \frac{d^3 T_0}{dZ^3} = 0. \quad (11)$$

On the other hand, if one evaluates the derivative with respect to  $Z$  of both sides of Eq. (9), one obtains

$$U_0 \frac{d^2 T_0}{dZ^2} - \alpha \frac{d^3 T_0}{dZ^3} = 0. \quad (12)$$

A comparison between Eqs. (11) and (12) allows one to conclude that either  $U$  is uniform in a duct cross-section or  $d^2 T_0/dZ^2$  is equal to zero. The former item can be ruled out since, on account of the absence of wall slip, it would imply the trivial case of a fluid at rest. Therefore, the non-trivial analysis which will be performed in the following is based on the condition  $d^2 T_0/dZ^2 = 0$ . In this case, Eq. (9) yields

$$\frac{dT_0}{dZ} = \frac{4\alpha \bar{q}_w}{kDU_0}, \quad (13)$$

and, as a consequence, Eq. (7) can be rewritten as

$$\frac{\partial^2 T}{\partial X^2} + \frac{\partial^2 T}{\partial Y^2} = \frac{4\bar{q}_w}{kDU_0} U. \quad (14)$$

Let us define the dimensionless quantities

$$\begin{aligned} t &= \frac{T - T_w}{\Delta T}, & u &= \frac{U}{U_0}, \\ x &= \frac{X}{a}, & y &= \frac{Y}{a}, & \sigma &= \frac{b}{a}, \\ Re &= \frac{U_0 D}{\nu}, & Gr &= \frac{g\beta\Delta T D^3}{\nu^2}, \\ \lambda &= -\frac{a^2}{\mu U_0} \frac{dP}{dZ}, & \eta &= \frac{T_0 - T_w}{\Delta T}, \end{aligned} \quad (15)$$

where  $\Delta T = \bar{q}_w D/k$  is the reference temperature difference. Obviously, since  $\partial T/\partial Z$  depends neither on  $X$  nor on  $Y$ , it coincides with  $dT_w/dZ$ . Therefore, the dimensionless temperature  $t$  depends only on  $x$  and on  $y$  and the dimensionless quantity  $\eta$  is a constant. On account of Eq. (15), Eqs. (2) and (14) can be rewritten as

$$\frac{\partial^2 u}{\partial x^2} + \frac{\partial^2 u}{\partial y^2} + \frac{(1+\sigma)^2}{4\sigma^2} \frac{Gr}{Re} (t - \eta) + \lambda = 0, \quad (16)$$

$$\frac{\partial^2 t}{\partial x^2} + \frac{\partial^2 t}{\partial y^2} - \frac{(1+\sigma)^2}{\sigma^2} u = 0. \quad (17)$$

The boundary conditions fulfilled by the dimensionless velocity  $u(x,y)$  and by the dimensionless temperature  $t(x,y)$  are as follows:

$$\begin{aligned} u(0,y) &= 0, & u(1,y) &= 0, \\ u(x,0) &= 0, & u(x,\sigma) &= 0, \end{aligned} \quad (18)$$

$$\begin{aligned} t(0,y) &= 0, & t(1,y) &= 0, \\ t(x,0) &= 0, & t(x,\sigma) &= 0. \end{aligned} \quad (19)$$

On account of Eqs. (5) and (10), two additional constraints must be fulfilled by the dimensionless functions  $u(x,y)$  and  $t(x,y)$ , namely

$$\int_0^1 dx \int_0^\sigma dy u(x,y) = \sigma, \quad (20)$$

$$\int_0^1 dx \int_0^\sigma dy t(x,y) = \sigma\eta. \quad (21)$$

The average wall shear stress is given by

$$\begin{aligned} \tau_{w,m} &= \frac{\mu}{2(a+b)} \left[ \int_0^b \frac{\partial U}{\partial X} \Big|_{X=0} dY - \int_0^b \frac{\partial U}{\partial X} \Big|_{X=a} dY \right. \\ &\quad \left. + \int_0^a \frac{\partial U}{\partial Y} \Big|_{Y=0} dX - \int_0^a \frac{\partial U}{\partial Y} \Big|_{Y=b} dX \right]. \end{aligned} \quad (22)$$

By employing Eq. (22), the Fanning friction factor can be expressed as

$$\begin{aligned} f &= \frac{2\tau_{w,m}}{\rho_0 U_0^2} \\ &= \frac{2\sigma}{(1+\sigma)^2 Re} \left[ \int_0^\sigma \frac{\partial u}{\partial x} \Big|_{x=0} dy - \int_0^\sigma \frac{\partial u}{\partial x} \Big|_{x=1} dy \right. \\ &\quad \left. + \int_0^1 \frac{\partial u}{\partial y} \Big|_{y=0} dx - \int_0^1 \frac{\partial u}{\partial y} \Big|_{y=\sigma} dx \right]. \end{aligned} \quad (23)$$

As a consequence of Eqs. (16) and (21), it is easily shown that a simple relation between the parameters  $f$  and  $\lambda$  occurs, namely

$$f Re = \frac{2\sigma^2 \lambda}{(1 + \sigma)^2}. \tag{24}$$

The peripherally averaged and axially local Nusselt number can be easily evaluated as

$$Nu = \frac{\bar{q}_w D}{(T_w - T_b)k} = \frac{\Delta T}{T_w - T_b} = -\frac{1}{t_b}, \tag{25}$$

where the bulk mean value of any quantity  $W$  is defined as

$$\begin{aligned} W_b &= \frac{1}{abU_0} \int_0^a dx \int_0^b dy W U \\ &= \frac{1}{\sigma} \int_0^1 dx \int_0^\sigma dy W u. \end{aligned} \tag{26}$$

Some authors [11,12] use an alternative definition of the Nusselt number based on the choice of  $T_0$  as the reference fluid temperature. This alternative definition may lead to less complicated mathematical expressions when dealing with mixed convection problems. Therefore, one may employ a parameter  $Nu_0$  given by

$$Nu_0 = \frac{\bar{q}_w D}{(T_w - T_0)k} = \frac{\Delta T}{T_w - T_0} = -\frac{1}{\eta}. \tag{27}$$

### 3. Analytical solution

The dimensionless velocity field  $u(x,y)$  and the dimensionless temperature  $t(x,y)$  can be evaluated by employing the finite Fourier transform method. The double finite Fourier sine transform of an arbitrary function  $R(x,y)$  in the rectangular domain  $\{0 \leq x \leq 1, 0 \leq y \leq \sigma\}$  is defined as [14]

$$\begin{aligned} \tilde{R}(n,m) &= \int_0^1 dx \int_0^\sigma dy R(x,y) \sin(n\pi x) \\ &\quad \times \sin\left(\frac{m\pi y}{\sigma}\right), \end{aligned} \tag{28}$$

where  $n$  and  $m$  are positive integers. By employing the properties of the finite Fourier sine transforms described in [14] and the boundary conditions given by Eqs. (18) and (19), Eqs. (16) and (17) can be rewritten as algebraic equations, namely

$$\begin{aligned} \left[ (n\pi)^2 + \left(\frac{m\pi}{\sigma}\right)^2 \right] \tilde{u} - \frac{(1 + \sigma)^2}{4\sigma^2} \frac{Gr}{Re} \tilde{t} \\ = \left[ \lambda - \frac{(1 + \sigma)^2}{4\sigma^2} \frac{Gr}{Re} \eta \right] \\ \times \frac{\sigma [1 - (-1)^n][1 - (-1)^m]}{nm\pi^2}, \end{aligned} \tag{29}$$

$$\left[ (n\pi)^2 + \left(\frac{m\pi}{\sigma}\right)^2 \right] \tilde{t} + \frac{(1 + \sigma)^2}{\sigma^2} \tilde{u} = 0. \tag{30}$$

The solution of Eqs. (29) and (30) is easily obtained and can be expressed as

$$\begin{aligned} \tilde{u}(n,m) \\ = \left[ \lambda - \frac{(1 + \sigma)^2}{4\sigma^2} \frac{Gr}{Re} \eta \right] \frac{\sigma [1 - (-1)^n][1 - (-1)^m]}{nm\pi^2} \\ \times \left\{ (n\pi)^2 + \left(\frac{m\pi}{\sigma}\right)^2 + \frac{(1 + \sigma)^4}{4\sigma^4 [(n\pi)^2 + (m\pi/\sigma)^2]} \frac{Gr}{Re} \right\}^{-1}, \end{aligned} \tag{31}$$

$$\tilde{t}(n,m) = -\frac{(1 + \sigma)^2}{(n\pi\sigma)^2 + (m\pi)^2} \tilde{u}(n,m). \tag{32}$$

On account of the inversion formula of double finite Fourier sine transforms [14]

$$R(x,y) = \frac{4}{\sigma} \sum_{n=1}^{\infty} \sum_{m=1}^{\infty} \tilde{R}(n,m) \sin(n\pi x) \sin\left(\frac{m\pi y}{\sigma}\right), \tag{33}$$

the constraints given by Eqs. (20) and (21) can be rewritten as

$$\sum_{n=1}^{\infty} \sum_{m=1}^{\infty} \frac{\tilde{u}(2n-1, 2m-1)}{(2n-1)(2m-1)} = \frac{\pi^2 \sigma}{16}, \tag{34}$$

$$\sum_{n=1}^{\infty} \sum_{m=1}^{\infty} \frac{\tilde{t}(2n-1, 2m-1)}{(2n-1)(2m-1)} = \frac{\pi^2 \sigma \eta}{16}. \tag{35}$$

Let us define the coefficients

$$C_{n,m} = \frac{4\tilde{u}(2n-1, 2m-1)\sigma^2}{4\lambda\sigma^2 - (1 + \sigma)^2 \eta Gr/Re}. \tag{36}$$

Eq. (31) allows one to conclude that  $C_{n,m}$  are independent of the unknown parameters  $\lambda$  and  $\eta$ . Therefore, as a consequence of Eqs. (32) and (34)–(36), the parameters  $\lambda$  and  $\eta$  can be determined by solving the set of equations

$$\begin{aligned} \sum_{n=1}^{\infty} \sum_{m=1}^{\infty} \frac{C_{n,m}}{(2n-1)(2m-1)} \\ = \frac{\pi^2 \sigma^3}{4[4\lambda\sigma^2 - (1 + \sigma)^2 \eta Gr/Re]}, \end{aligned} \tag{37}$$

$$\begin{aligned} \sum_{n=1}^{\infty} \sum_{m=1}^{\infty} \frac{C_{n,m}}{[(2n-1)^2 \sigma^2 + (2m-1)^2](2n-1)(2m-1)} \\ = -\frac{\pi^4 \sigma^3 \eta}{4(1 + \sigma)^2 [4\lambda\sigma^2 - (1 + \sigma)^2 \eta Gr/Re]}. \end{aligned} \tag{38}$$

For prescribed values of  $\sigma$  and  $Gr/Re$ , Eqs. (37) and (38) yield the following expressions of  $\lambda$  and  $\eta$ :

$$\lambda = \frac{\pi^4 \sigma^3 - 4Gr/Re(1 + \sigma)^4 F_2}{16\pi^2 \sigma^2 F_1}, \tag{39}$$

$$\eta = -\frac{(1+\sigma)^2 F_2}{\pi^2 F_1}, \quad (40)$$

where the dimensionless parameters  $F_1$  and  $F_2$  are defined as

$$F_1 = \sum_{n=1}^{\infty} \sum_{m=1}^{\infty} \frac{C_{n,m}}{(2n-1)(2m-1)}, \quad (41)$$

$$F_2 = \sum_{n=1}^{\infty} \sum_{m=1}^{\infty} \frac{C_{n,m}}{[(2n-1)^2\sigma^2 + (2m-1)^2](2n-1)(2m-1)}. \quad (42)$$

On account of Eqs. (25), (26), (32), (33) and (36), the Nusselt number  $Nu$  can be evaluated by employing the expression

$$\begin{aligned} \frac{1}{Nu} &= -t_b = -\frac{4}{\sigma^2} \sum_{n=1}^{\infty} \sum_{m=1}^{\infty} \tilde{u}(n,m) \tilde{t}(n,m) \\ &= \left[ 4\lambda\sigma^2 - (1+\sigma)^2 \eta \frac{Gr}{Re} \right]^2 \frac{(1+\sigma)^2}{4\pi^2\sigma^6} \\ &\quad \times \sum_{n=1}^{\infty} \sum_{m=1}^{\infty} \frac{C_{n,m}^2}{(2n-1)^2\sigma^2 + (2m-1)^2}. \end{aligned} \quad (43)$$

As one can easily verify, Eqs. (24), (27), (31), (36) and (39)–(43) allow one to conclude that the dimensionless parameters  $fRe$ ,  $\eta$ ,  $Nu$  and  $Nu_0$  are left invariant by the change  $\sigma \rightarrow 1/\sigma$ . This feature is quite expected since the boundary conditions are the same on the four walls of the duct and the change  $\sigma \rightarrow 1/\sigma$  does not alter the shape of the duct cross-section. Therefore, in the following, the values of the parameters  $fRe$ ,  $\eta$ ,  $Nu$  and  $Nu_0$  will be considered only in the interval  $0 < \sigma \leq 1$ .

According to Eqs. (31) and (32), the dimensionless velocity  $u$  and, as a consequence, the dimensionless temperature  $t$  are ill defined in correspondence with an infinite sequence of negative values of  $Gr/Re$  defined by

$$\frac{Gr}{Re} = -\frac{4\pi^4[(2n-1)^2\sigma^2 + (2m-1)^2]^2}{(1+\sigma)^4}, \quad (44)$$

for every positive integer value of both  $n$  and  $m$ . The sequence defined by Eq. (44) is monotonically decreasing. According to Eq. (44), the smallest absolute value of  $Gr/Re$  corresponding to a singular solution ranges from  $\pi^4$  for  $\sigma = 1$  to  $4\pi^4$  for  $\sigma \rightarrow 0$ . Indeed, if  $Gr/Re$  is given by Eq. (44) for a pair of positive integers  $n_0$  and  $m_0$ , Eqs. (29) and (30) allow one to come to the following conclusions:

- $\lambda = (Gr/Re)\eta(1+\sigma)^2/4\sigma^2$ ;
- $\tilde{u}(n,m)$  and  $\tilde{t}(n,m)$  are zero unless both  $n = 2n_0 - 1$  and  $m = 2m_0 - 1$ ;
- Eq. (34) implies that  $\tilde{u}(2n_0 - 1, 2m_0 - 1) = \pi^2\sigma(2n_0 - 1)(2m_0 - 1)/16$ ;
- $\tilde{t}(2n_0 - 1, 2m_0 - 1)$  can be obtained by employing Eq. (32);

- Eq. (35) implies that  $\eta = 16\tilde{t}(2n_0 - 1, 2m_0 - 1)/[\pi^2\sigma(2n_0 - 1)(2m_0 - 1)]$ .

Stated differently, when Eq. (44) is fulfilled,  $-(Gr/Re)(1+\sigma)^4/4\sigma^4$  is an eigenvalue of the biharmonic operator  $\nabla^4$  in the two-dimensional rectangular domain  $\{0 \leq x \leq 1, 0 \leq y \leq \sigma\}$ . Moreover, Eqs. (16) and (17) show that the dimensionless velocity  $u(x,y)$  is the eigenfunction of  $\nabla^4$  corresponding to this eigenvalue. To summarize, when Eq. (44) holds, the infinite sum given by the inversion formula (33) to express either  $u(x,y)$  or  $t(x,y)$  collapses to a single term. However, as can be easily checked, neither the distributions  $u(x,y)$  and  $t(x,y)$  nor the parameters  $\lambda$ ,  $\eta$ ,  $fRe$ ,  $Nu$  and  $Nu_0$  undergo any discontinuity with respect to  $Gr/Re$  in the neighbourhood of an eigenvalue defined by Eq. (44), so that no special physical significance seems to be connected with these eigenvalues. Indeed, in the following sections, it will be shown that the first eigenvalue of the sequence defined by Eq. (44) plays a special role in the formulation of the necessary condition for the onset of flow reversal.

A quite interesting case is the limit  $dP/dZ \rightarrow 0$ , which corresponds to a purely buoyancy-driven flow, i.e. to free convection. In this limit, both the parameters  $\lambda$  and  $fRe$  tend to 0. For any prescribed aspect ratio  $\sigma$ , Eq. (39) reveals that the condition  $\lambda \rightarrow 0$  corresponds to a special value of the ratio  $Gr/Re$ , which can be determined as the root of the following equation:

$$\frac{\pi^4\sigma^3}{4} - \frac{Gr}{Re}(1+\sigma)^4 F_2 = 0. \quad (45)$$

Any root,  $Gr/Re$ , of Eq. (45) corresponds to a non-vanishing value of the mean velocity which can be obtained by utilizing the relation  $U_0 = (Re/Gr)(g\beta\Delta T D^2/\nu)$ . However, if one fixes the value of  $\sigma$ , it is easily verified that, starting from  $Gr/Re = 0$  and decreasing continuously the value of  $Gr/Re$ , one first encounters a root of Eq. (45), i.e. a free convection solution, and then a zero of  $F_1$ , i.e. a singularity of the parameters  $\lambda$ ,  $\eta$ ,  $fRe$ ,  $Nu$  and  $Nu_0$  as well as of the distributions  $u(x,y)$  and  $t(x,y)$ . The former, namely the root of Eq. (45), is denoted by  $(Gr/Re)''$  and the latter, namely the zero of  $F_1$ , is denoted by  $(Gr/Re)'''$ . By definition, both these values are negative. In Table 1, values of  $(Gr/Re)''$  and  $(Gr/Re)'''$  are reported for  $\sigma$  ranging from 0.1 to 1.0. Since the values of  $(Gr/Re)''$  are negative, the residual mean velocity  $U_0$  associated to the free convection solution is negative in the case of fluid heating ( $\bar{q}_w > 0$ ) and positive in the case of fluid cooling ( $\bar{q}_w < 0$ ).

Finally, it should be pointed out that, in the limit  $Gr/Re \rightarrow 0$ , i.e. in the limit of forced convection, Eqs. (31) and (33) yield a dimensionless velocity distribution  $u(x,y)$  coincident with that reported in [15].

Table 1  
Values of  $(Gr/Re)'$ ,  $(Gr/Re)''$ ,  $(Gr/Re)'''$ ,  $Nu'$  and  $(Gr/Re)_t$

| $\sigma$ | $(Gr/Re)'$ | $(Gr/Re)''$ | $(Gr/Re)'''$ | $Nu'$    | $(Gr/Re)_t$ |
|----------|------------|-------------|--------------|----------|-------------|
| 0.1      | -271.48    | -310.66     | -311.27      | 0.011134 | -289.77     |
| 0.2      | -203.24    | -318.23     | -328.51      | 0.21989  | -265.01     |
| 0.3      | -162.08    | -341.74     | -399.89      | 1.0950   | -285.77     |
| 0.4      | -136.48    | -338.27     | -507.45      | 1.9992   | -337.80     |
| 0.5      | -120.26    | -319.20     | -637.86      | 2.3684   | -410.61     |
| 0.6      | -109.97    | -300.93     | -777.84      | 2.4886   | -493.25     |
| 0.7      | -103.57    | -287.67     | -912.83      | 2.5261   | -573.40     |
| 0.8      | -99.829    | -279.35     | -1026.2      | 2.5367   | -638.59     |
| 0.9      | -97.950    | -275.03     | -1100.6      | 2.5392   | -679.22     |
| 1.0      | -97.409    | -273.77     | -1125.2      | 2.5396   | -692.18     |

4. Discussion of the results: friction factor and Nusselt number

As has been shown in the preceding section, Eqs. (24), (27), (31)–(33), (36) and (39)–(43) allow the evaluation of the dimensionless distributions  $u(x, y)$ ,  $t(x, y)$  and of the dimensionless parameters  $\lambda$ ,  $\eta$ ,  $fRe$ ,  $Nu$  and  $Nu_0$ , for any prescribed value of  $\sigma$  and  $Gr/Re$ .

Some comparisons can be made between the solution obtained in the preceding section and other solutions available in the literature for similar geometries and boundary conditions.

A quite instructive comparison can be performed by analysing the solution for the same geometry and for the same thermal boundary conditions presented in [3]. Indeed, Han [3] considers a condition of fully developed flow as well as the Boussinesq approximation. The only difference between the hypotheses made in [3] and those made in the present paper is in the choice of the reference temperature for the linearization of the equation of state  $\varrho = \varrho(T)$ . While in the present paper this reference temperature is chosen as the mean temperature  $T_0$  in a duct section, Han [3] chooses the wall temperature  $T_w$ . Both  $T_0$  and  $T_w$  change linearly in the  $Z$ -direction. Then, while in the present paper the change in the  $Z$ -direction of the reference mass density  $\varrho(T_0)$  is neglected, in Han’s paper the change in the  $Z$ -direction of the reference mass density  $\varrho(T_w)$  is neglected. As a consequence, a comparison between the solution found in the present paper and that found by Han [3] allows one to value the importance of the choice of the reference temperature in developing theoretical predictions of mixed convection flows. An extended investigation on this subject referring to plane-parallel channel flows can be found in [13]. Table 2 displays the above-mentioned comparison between Han’s solution and the present paper’s solution. More precisely, the comparison is performed by considering values of the dimensionless parameters  $fRe$  and  $Nu$  for a square duct,  $\sigma = 1$ . Table 2 shows that the discrepancies with the values reported by Han [3] for positive values of  $Gr/Re$  increase with  $Gr/Re$  and are specially strong for the parameter  $fRe$ . For instance, if

Table 2  
Values of  $fRe$  and  $Nu$  for a square duct,  $\sigma = 1$

| $Gr/Re$    | $fRe$         |          | $Nu$          |          |
|------------|---------------|----------|---------------|----------|
|            | Present paper | Ref. [3] | Present paper | Ref. [3] |
| 0          | 14.227        | 14.23    | 3.6080        | 3.61     |
| $\pi^4/4$  | 15.226        | 17.565   | 3.6965        | 3.69     |
| 50         | 16.244        | –        | 3.7884        | –        |
| 150        | 19.913        | –        | 4.1338        | –        |
| $5\pi^4/2$ | 22.983        | 45.365   | 4.4380        | 4.27     |
| 250        | 23.185        | –        | 4.4584        | –        |
| 350        | 26.137        | –        | 4.7627        | –        |
| 450        | 28.829        | –        | 5.0473        | –        |
| 550        | 31.305        | –        | 5.3136        | –        |
| 650        | 33.600        | –        | 5.5626        | –        |
| 750        | 35.741        | –        | 5.7958        | –        |
| 850        | 37.751        | –        | 6.0145        | –        |
| 950        | 39.647        | –        | 6.2198        | –        |
| 1050       | 41.444        | –        | 6.4129        | –        |
| $25\pi^4$  | 60.320        | 220.9    | 8.2786        | 9.46     |

$Gr/Re = 25\pi^4 \simeq 2435.2$ , the value of  $fRe$  predicted by Han is almost four times that found in the present paper. There is an agreement with the analysis performed in [13], where it is pointed out that the friction factor is a parameter which is very sensitive to the choice of reference temperature.

Another interesting comparison can be made by considering the limit  $\sigma \rightarrow 0$ . In this limit, Eqs. (24), (27), (31), (36), (39) and (40) yield

$$fRe = \left\{ \pi^2 - 8 \frac{Gr}{Re} \sum_{n=1}^{\infty} \frac{1}{(2n-1)^2 [4(2n-1)^4 \pi^4 + Gr/Re]} \right\} \times \left\{ 16\pi^2 \sum_{n=1}^{\infty} \frac{1}{4(2n-1)^4 \pi^4 + Gr/Re} \right\}^{-1}, \quad (46)$$

$$Nu_0 = \pi^2 \left\{ \sum_{n=1}^{\infty} \frac{1}{(2n-1)^2 [4(2n-1)^4 \pi^4 + Gr/Re]} \right\}^{-1} \times \sum_{n=1}^{\infty} \frac{1}{4(2n-1)^4 \pi^4 + Gr/Re}. \quad (47)$$

The values of  $fRe$  and  $Nu_0$  obtained by Eqs. (46) and (47) are expected to coincide with those obtained for a parallel-plate channel. Indeed, for the latter geometry, a closed-form solution of the momentum and energy balance equations exists, expressed in terms of trigonometric and hyperbolic functions [12,16]. The special symmetry of the parallel-plate channel implies that this solution can be employed both for the H1 boundary conditions and for the H2 boundary conditions. It is easily verified that an approximate evaluation of  $fRe$  and  $Nu_0$  obtained by employing Eqs. (46) and (47) with sums truncated to 200 terms is sufficient to obtain a complete agreement with the values of these quantities tabulated in [12].

Finally, an important comparison can be made by considering the limit  $Gr/Re \rightarrow 0$ , i.e. the special case of forced convection. As has been pointed out in the preceding section, in the limit  $Gr/Re \rightarrow 0$ , the dimensionless velocity distribution  $u(x, y)$  evaluated through Eqs. (31) and (33) agrees exactly with the fully developed velocity distribution for isothermal flow in a rectangular duct reported in [15]. Moreover, in this limit, also the dimensionless parameter  $\lambda$  expressed by Eq. (39) coincides with that evaluated by employing the results for isothermal flow obtained in [15]. In [2], a correlation which allows one to evaluate  $Nu$  for a given aspect ratio  $\sigma$  is reported for the case of laminar forced convection with H1 boundary conditions, namely

$$Nu = 8.235(1 - 2.0421\sigma + 3.0853\sigma^2 - 2.4765\sigma^3 + 1.0578\sigma^4 - 0.1861\sigma^5). \quad (48)$$

By employing Table 3, the values of  $Nu$  evaluated through Eq. (43) can be compared with those which can be obtained by the correlation which appears in Eq. (48). Table 3 shows that there exists a very fair agreement between the values obtained through Eq. (43) and those evaluated by the correlation reported in [2], the relative discrepancy being less than 0.085%.

Tables 2, 4 and 5 display values of  $fRe$  and  $Nu$  referring to  $\sigma = 1$  (square duct) and  $\sigma = 0.5$  both for

Table 3  
Values of  $Nu$  in the case of forced convection,  $Gr/Re \rightarrow 0$

| $\sigma$ | $Nu$          |          |
|----------|---------------|----------|
|          | Present paper | Ref. [2] |
| 0.1      | 6.7850        | 6.7879   |
| 0.2      | 5.7377        | 5.7383   |
| 0.3      | 4.9899        | 4.9929   |
| 0.4      | 4.4719        | 4.4756   |
| 0.5      | 4.1233        | 4.1258   |
| 0.6      | 3.8946        | 3.8963   |
| 0.7      | 3.7496        | 3.7518   |
| 0.8      | 3.6638        | 3.6665   |
| 0.9      | 3.6205        | 3.6231   |
| 1.0      | 3.6080        | 3.6102   |

Table 4  
Values of  $fRe$  and  $Nu$  for a square duct,  $\sigma = 1$

| $Gr/Re$ | $fRe$   | $Nu$     |
|---------|---------|----------|
| -50     | 12.068  | 3.4225   |
| -150    | 7.2339  | 3.0376   |
| -250    | 1.5208  | 2.6367   |
| -350    | -5.4068 | 2.2248   |
| -450    | -14.083 | 1.8095   |
| -550    | -25.411 | 1.4015   |
| -650    | -41.057 | 1.0147   |
| -750    | -64.461 | 0.66584  |
| -850    | -104.06 | 0.37346  |
| -950    | -187.56 | 0.15605  |
| -1050   | -489.90 | 0.029275 |

Table 5  
Values of  $fRe$  and  $Nu$  for  $\sigma = 0.5$

| $Gr/Re$ | $fRe$   | $Nu$    |
|---------|---------|---------|
| -550    | -47.378 | 0.33753 |
| -450    | -14.420 | 1.2143  |
| -350    | -2.4858 | 2.1200  |
| -250    | 4.5707  | 2.8657  |
| -150    | 9.6696  | 3.4526  |
| -50     | 13.753  | 3.9215  |
| 0       | 15.548  | 4.1233  |
| 50      | 17.220  | 4.3081  |
| 150     | 20.275  | 4.6370  |
| 250     | 23.029  | 4.9247  |
| 350     | 25.555  | 5.1818  |
| 450     | 27.899  | 5.4157  |
| 550     | 30.093  | 5.6312  |
| 650     | 32.161  | 5.8319  |
| 750     | 34.121  | 6.0204  |
| 850     | 35.987  | 6.1985  |
| 950     | 37.770  | 6.3676  |
| 1050    | 39.479  | 6.5288  |

positive and for negative values of the ratio  $Gr/Re$ . It must be pointed out that the discussion of the case  $Gr/Re < 0$  needs some additional care. In fact, it has been shown in the preceding section that, when  $Gr/Re < 0$ , the solution displays singularities. For a fixed  $\sigma$ , the singularity with the smallest absolute value of  $Gr/Re$  is encountered for  $Gr/Re = (Gr/Re)'''$ . Values of  $(Gr/Re)'''$  for different values of  $\sigma$  have been reported in Table 1. A similar circumstance has been already detected for fully developed and laminar mixed convection in uniformly heated ducts with non-rectangular geometries, as, for instance, in the case of a circular duct [11] and in the case of a parallel-plate channel [12]. Although, to my knowledge, no rigorous proof exists, the singularity with the smallest absolute value of  $Gr/Re$  can be somewhat connected to the breakdown of the stability of the laminar solution [11,12]. Further investigations in this direction would require a stability analysis of the laminar velocity and temperature distri-



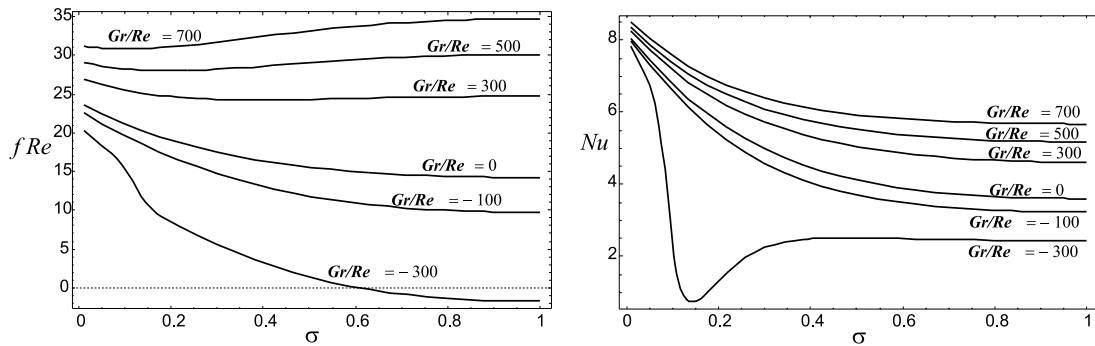


Fig. 2. Plots of  $fRe$  and  $Nu$  vs  $\sigma$ .

butions, which is beyond the aims of the present paper. However, in the following, the study for negative values of  $Gr/Re$  will be restricted to the interval  $(Gr/Re)^{''' < Gr/Re < 0$ . Tables 2, 4 and 5 reveal that both  $fRe$  and  $Nu$  are strictly increasing functions of the ratio  $Gr/Re$ . In particular, Tables 4 and 5 clearly show the change of sign which affects  $fRe$  for  $Gr/Re = (Gr/Re)''$ . Indeed, the values of  $fRe$  are negative for  $(Gr/Re)^{''' < Gr/Re < (Gr/Re)''$ . A negative value of  $fRe$  can be ascribed to the occurrence of flow reversal next to the duct walls, for the following reason. As can be inferred by means of Eq. (23), a negative value of  $fRe$  implies a negative average wall value of the component of  $\nabla u$  along the inward normal direction. Then, there exist regions next to the duct walls where  $u$  is negative and this corresponds to flow reversal. Obviously, this conclusion should not lead to the wrong deduction that flow reversal occurs *only* when  $fRe < 0$ . The necessary condition for the onset of flow reversal will be discussed in the next section.

In Fig. 2, plots of  $fRe$  and of  $Nu$  versus  $\sigma$  are reported for various values of  $Gr/Re$ . This figure shows that, while in the case of forced convection both  $fRe$  and  $Nu$  are decreasing functions of the aspect ratio  $\sigma$ , the behaviour of these parameters may be non-monotonic for mixed convection and depends strongly on the ratio  $Gr/Re$ . Specially evident is the local minimum which characterizes the dependence of  $Nu$  on  $\sigma$  for  $Gr/Re = -300$ . Moreover, it can be pointed out that, for  $Gr/Re = -300$ , the parameter  $fRe$  becomes zero when  $\sigma \approx 0.6$ , and is negative when  $\sigma$  is approximately greater than 0.6. In this range, flow reversal is expected to occur. Finally, as is shown especially by the plots of  $fRe$ , the effect of buoyancy is enhanced as the aspect ratio increases.

**5. Discussion of the results: velocity and temperature distributions**

On account of Eqs. (31)–(33), (36), (37) and (41), the dimensionless velocity  $u(x, y)$  and the dimensionless temperature  $t(x, y)$  can be expressed as follows:

$$u(x, y) = \frac{\pi^2}{4F_1} \sum_{n=1}^{\infty} \sum_{m=1}^{\infty} C_{n,m} \sin[(2n - 1)\pi x] \times \sin \left[ \frac{(2m - 1)\pi y}{\sigma} \right], \tag{49}$$

$$t(x, y) = -\frac{(1 + \sigma)^2}{4F_1} \times \sum_{n=1}^{\infty} \sum_{m=1}^{\infty} \frac{C_{n,m} \sin[(2n - 1)\pi x]}{(2n - 1)^2 \sigma^2 + (2m - 1)^2} \times \sin \left[ \frac{(2m - 1)\pi y}{\sigma} \right]. \tag{50}$$

As can be inferred by an analysis of the dimensionless velocity behaviour as implied by Eq. (49), for a fixed aspect ratio  $\sigma$  there exists a negative real number,  $(Gr/Re)'$ , such that flow reversal occurs whenever  $Gr/Re < (Gr/Re)'$ . In particular, the onset of flow reversal takes place at the four corners between neighbouring walls, namely next to the positions  $(0, 0)$ ,  $(0, \sigma)$ ,  $(1, \sigma)$  and  $(1, 0)$ . This circumstance is illustrated in Fig. 3, where plots of the distribution of the dimensionless velocity  $u$  either on the plane  $x = 0.05$  or on the plane  $y = 0.01$  are reported for different negative values of  $Gr/Re$ , with reference to the aspect ratio  $\sigma = 0.5$ . Strictly speaking, flow reversal occurs if there exists a domain where the dimensionless velocity  $u$  is negative. On account of the no-slip condition at the walls, it is easily shown that the onset of flow reversal in a neighbourhood of one of the four corners between neighbouring walls is accompanied by a sign change of the derivative  $\partial^2 u / \partial x \partial y$  evaluated at that corner. Obviously, the symmetry of the solution implies that the onset of flow reversal is simultaneous at the four corners, so that one can perform the analysis with reference to the corner  $(0, 0)$ . Then, the onset of flow reversal implies that the sign of the derivative  $\partial^2 u / \partial x \partial y$  in a small neighbourhood of  $(0, 0)$  changes from positive to negative. By employing Eqs. (31), (36) and (49), this derivative can be expressed as

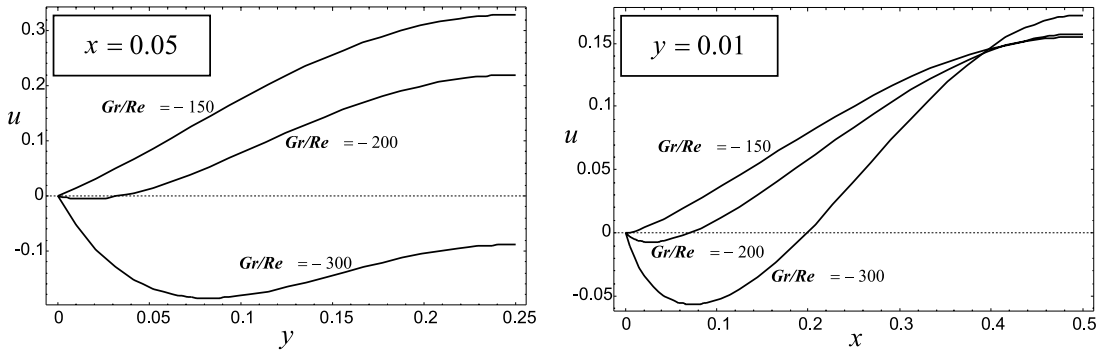


Fig. 3. Plots of  $u$  vs  $y$  for  $x = 0.05$  (upper frame) and of  $u$  vs  $x$  for  $y = 0.01$  (lower frame), in the case  $\sigma = 0.5$ .

$$\begin{aligned} & \frac{\partial^2 u(x,y)}{\partial x \partial y} \\ &= \frac{4\pi^4 \sigma^2}{F_1} \sum_{n=1}^{\infty} \sum_{m=1}^{\infty} [(2n-1)^2 \sigma^2 + (2m-1)^2] \cos[(2n-1)\pi x] \\ & \quad \times \{4\pi^4 [(2n-1)^2 \sigma^2 + (2m-1)^2]^2 + (1+\sigma)^4 Gr/Re\}^{-1} \\ & \quad \times \cos\left[\frac{(2m-1)\pi y}{\sigma}\right]. \end{aligned} \tag{51}$$

As is shown by Eq. (51), the derivative  $\partial^2 u/\partial x \partial y$  becomes singular in the limit  $(x,y) \rightarrow (0,0)$ . Indeed, in this limit, the double sum which appears in Eq. (51) tends to  $+\infty$ , so that the sign of  $\partial^2 u/\partial x \partial y$  in a small neighbourhood of  $(0,0)$  coincides with the sign of the quantity  $F_1$ . As is shown by Eqs. (31), (36) and (41),  $F_1$  is a function of  $\sigma$  and  $Gr/Re$ . These equations reveal that, if  $\sigma$  is fixed, the quantity  $F_1$  is positive for  $-4\pi^4(1+\sigma^2)^2/(1+\sigma)^4 < Gr/Re < 0$  and is singular for  $Gr/Re = -4\pi^4(1+\sigma^2)^2/(1+\sigma)^4$ . This singularity leads to a sign change and this sign change leads to the onset of flow reversal. Then, the quantity  $(Gr/Re)'$  is given by

$$\left(\frac{Gr}{Re}\right)' = -\frac{4\pi^4(1+\sigma^2)^2}{(1+\sigma)^4}. \tag{52}$$

To summarize,  $(Gr/Re)'$  is the value of  $Gr/Re$  below which flow reversal occurs, the onset of this phenomenon being located next to the four corners between neighbouring walls, namely the positions  $(0,0)$ ,  $(0,\sigma)$ ,  $(1,\sigma)$  and  $(1,0)$ . Obviously,  $(Gr/Re)'$  is the smallest term of the sequence defined by Eq. (44). Values of  $(Gr/Re)'$  for different aspect ratios are reported in Table 1. This table contains somewhat a summary of the features which characterize the flow for a fixed aspect ratio, in the case  $Gr/Re < 0$ . If  $(Gr/Re)' < Gr/Re < 0$ , no flow reversal occurs. If  $(Gr/Re)'' < Gr/Re < (Gr/Re)'$ , flow reversal occurs and buoyancy becomes dominant, until flow is purely buoyancy driven when  $Gr/Re = (Gr/Re)''$ . If  $(Gr/Re)''' < Gr/Re < (Gr/Re)''$ , the local values of the dimensionless velocity and temperature as well as the

parameters  $\lambda$ ,  $\eta$  and  $Nu$  undergo increasingly rapid changes with  $Gr/Re$  and become singular for  $Gr/Re = (Gr/Re)'''$ . As is shown in Table 1, the absolute value of  $(Gr/Re)'$  decreases monotonically with  $\sigma$ , i.e. the onset of flow reversal is assisted if the aspect ratio increases.

The distributions  $u(x,y)$  and  $t(x,y)$  are plotted for a square duct ( $\sigma = 1$ ) in Figs. 4 and 6. In particular, Fig. 4 refers to  $Gr/Re = 1000$ , while Fig. 6 refers to the case  $Gr/Re = -1000$ . The case considered in Fig. 4 corresponds either to upward flow ( $U_0 > 0$ ) in a heated duct ( $\bar{q}_w > 0$ ) or to downward flow ( $U_0 < 0$ ) in a cooled duct ( $\bar{q}_w < 0$ ). With reference to the first circumstance, the four local maxima of  $u(x,y)$  displayed in Fig. 4 can be interpreted as flow enhancement next to a corner between neighbouring heated walls. Moreover, by considering upward flow in a heated duct, the local minimum of  $u(x,y)$  corresponding to the centre  $(0.5,0.5)$  represents the minimum velocity associated to a point of minimum temperature (and, hence, of maximum density). Indeed, Fig. 4 shows that the dimensionless temperature  $t$  displays a minimum at the position  $(0.5,0.5)$ . Although the local minimum of  $u(x,y)$  corresponding to the centre  $(0.5,0.5)$  for  $Gr/Re = 1000$  is not visible in Fig. 4, it is represented markedly in Fig. 5. The latter figure shows the behaviour of  $u$  versus  $x$  for fixed values of  $y$ , with reference to a square duct with  $Gr/Re = 1000$ , i.e. for the same case as examined in Fig. 4.

An analysis of Fig. 6 reveals two relevant features of the distributions  $u(x,y)$  and  $t(x,y)$  for  $Gr/Re = -1000$ : flow reversal and the occurrence of positive values of  $t$ . The former feature is quite expected on account of the investigation on flow reversal performed at the beginning of this section. Indeed, by employing Table 1, one expects flow reversal to occur in a square duct for any value of  $Gr/Re$  lower than  $-97.409$ . On the other hand, the occurrence of values of  $t$  greater than zero is a somewhat unexpected and interesting feature which can be interpreted as follows. The case considered in Fig. 6 corresponds either to upward flow ( $U_0 > 0$ ) in a cooled

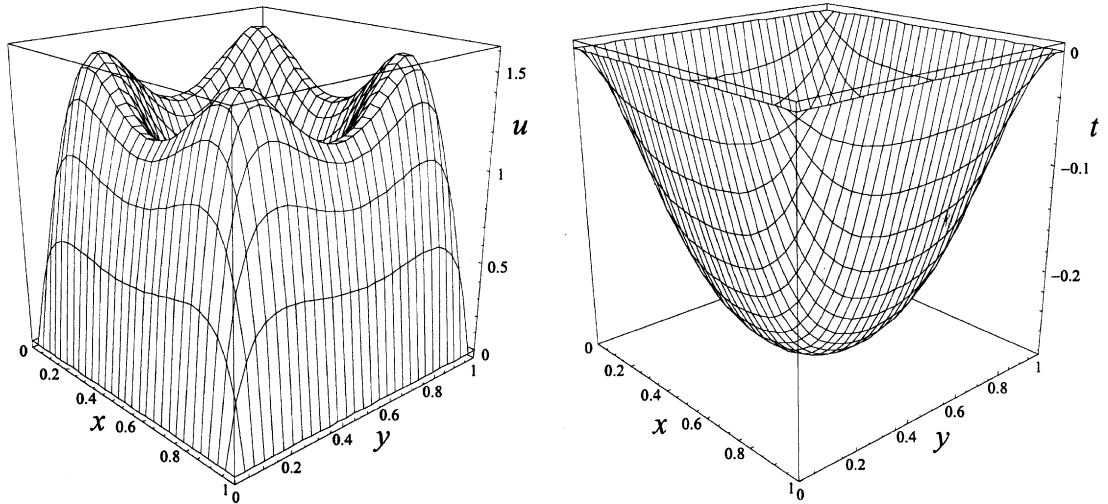


Fig. 4. Plots of  $u(x, y)$  (upper frame) and  $t(x, y)$  (lower frame) for  $\sigma = 1$  and  $Gr/Re = 1000$ .

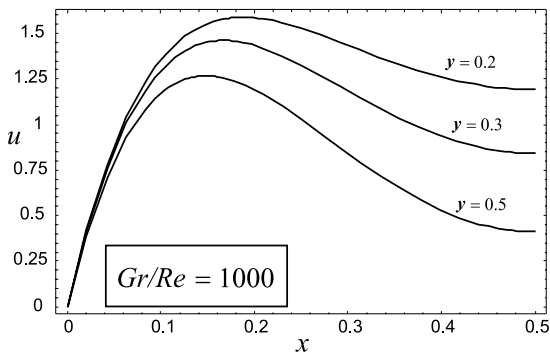


Fig. 5. Plots of  $u$  vs  $x$  for different values of  $y$ , in the case of a square duct ( $\sigma = 1$ ) with  $Gr/Re = 1000$ .

duct ( $\bar{q}_w < 0$ ) or to downward flow ( $U_0 < 0$ ) in a heated duct ( $\bar{q}_w > 0$ ). Then, as is easily shown by employing Eq. (15), if one assumes that downward flow in a heated duct occurs, the condition  $t > 0$  implies that there exist positions within a duct cross-section where  $T > T_w$ . Obviously, this is not a violation of the second law. In fact, for any choice of the axial position  $Z$ , it is always possible to find another axial position  $Z'$  such that  $T_w(Z') > T(X, Y, Z)$ , even if  $X$  and  $Y$  are such that  $T(X, Y, Z) > T_w(Z)$ . On the other hand, as is explained in the following, the above effect is governed by the H1 boundary conditions which imply a linear axial change of the wall temperature  $T_w$ . Indeed, the existence of positions where  $t > 0$  is merely a consequence of an

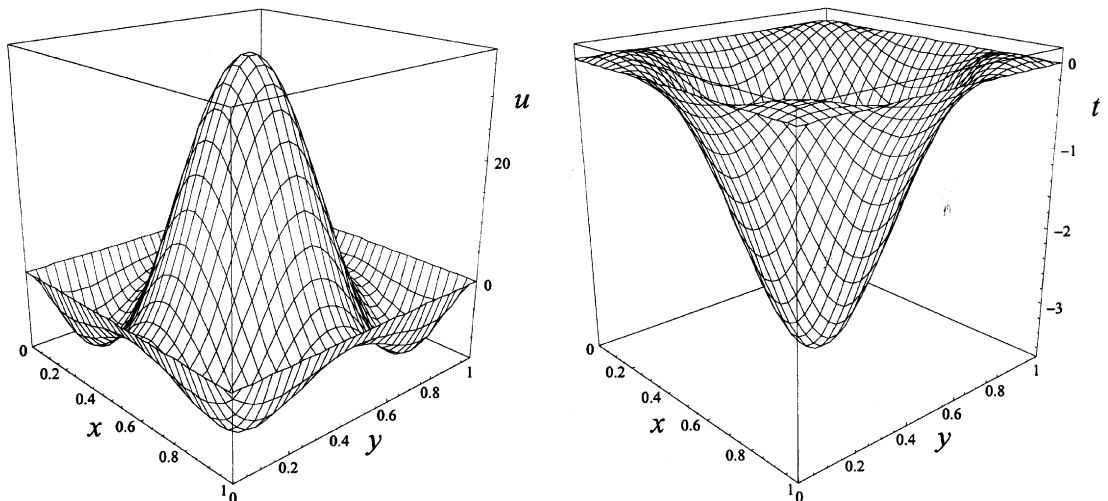


Fig. 6. Plots of  $u(x, y)$  (upper frame) and  $t(x, y)$  (lower frame) for a square duct ( $\sigma = 1$ ) and  $Gr/Re = -1000$ .

extremely intense flow reversal. The effect of flow reversal produces an axial heat transfer in a direction opposite to the net fluid flow and, as a consequence, an extra fluid heating. In other words, the fluid experiences a *pre-heating* (in the case of a heated duct) or a *pre-cooling* (in the case of a cooled duct) induced by flow reversal.

As is well known, in fully developed duct flow convection, the occurrence of temperature fields which do not undergo a monotonic change moving from the wall to the centre of the duct cross-section is usually connected to phenomena of internal heat generation such as viscous dissipation [17,18]. From a strictly mathematical viewpoint, the effect of flow reversal can be compared to a heat generation, as can be easily checked by an analysis of Eq. (14). This equation shows that, for a heated duct, the axial convection term is analogous to a heat generation term. According to this analogy, the equivalent power generated is negative for direct flow ( $U/U_0 > 0$ ) and positive for reversed flow ( $U/U_0 < 0$ ). A more apparent representation of the occurrence of positive dimensionless temperatures can be found in Fig. 7, which also refers to a square duct ( $\sigma = 1$ ). In this figure, three different plots of  $t(x, 0.1)$  versus  $x$  are reported for  $Gr/Re = -1100, -1070$  and  $-1000$ . In all the examined cases, positive values of  $t$  are displayed in the region next to the wall  $x = 0$ . As can be checked out in Table 1, the ratios  $Gr/Re$  considered in this figure are very close to the value of  $(Gr/Re)'''$  for a square duct, i.e.  $-1125.2$ . As has been pointed out in the preceding sections, when  $Gr/Re = (Gr/Re)'''$ , both the distributions  $u(x, y)$  and  $t(x, y)$  become singular. This explains the increasing sensitivity of the dimensionless velocity field and of the dimensionless temperature field to changes of  $Gr/Re$ .

Fig. 6 shows that the onset of the effect of pre-heating (pre-cooling), namely the occurrence of positive values of  $t$ , takes place next to the four corners between neighbouring walls. Then, the necessary and sufficient condition for the onset of this effect can be determined

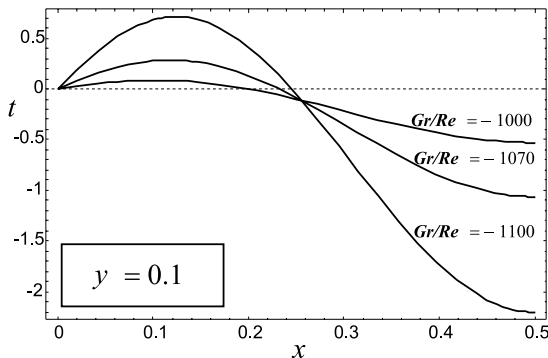


Fig. 7. Plots of  $t$  vs  $x$  for  $y = 0.1$ , in the case of a square duct ( $\sigma = 1$ ).

by a method similar to that invoked for the onset of flow reversal. One can easily conclude that positive values of  $t$  exist only when the derivative  $\partial^2 t / \partial x \partial y$  evaluated at  $(0, 0)$  becomes positive. Therefore, for any fixed value of  $\sigma$  there exists a negative real number  $(Gr/Re)_t$  such that positive values of  $t$  occur if and only if  $Gr/Re < (Gr/Re)_t$ . Obviously, on account of Eqs. (31), (36) and (50), the values of  $(Gr/Re)_t$  for a given  $\sigma$  can be obtained by determining the zeros of

$$\begin{aligned} \frac{\partial^2 t}{\partial x \partial y} \Big|_{x=0, y=0} &= -\frac{4\pi^2 \sigma^2 (1 + \sigma)^2}{F_1} \\ &\times \sum_{n=1}^{\infty} \sum_{m=1}^{\infty} 1 / \{4\pi^4 [(2n - 1)^2 \sigma^2 + (2m - 1)^2]^2 \\ &+ (1 + \sigma)^4 Gr/Re\}. \end{aligned} \tag{53}$$

Values of  $(Gr/Re)_t$  for different aspect ratios  $\sigma$  are reported in Table 1. This table shows that  $(Gr/Re)_t > (Gr/Re)''$  for small values of  $\sigma$ , so that the free convection solution displays the pre-heating (pre-cooling) effect. On the other hand, for values of  $\sigma$  approximately greater than 0.4 and smaller than 1,  $(Gr/Re)_t$  is such that  $(Gr/Re)'' > (Gr/Re)_t > (Gr/Re)'''$ .

It must be pointed out that the effect of pre-heating (pre-cooling) does not occur in the limiting case  $\sigma \rightarrow 0$ , i.e. for a parallel-plate channel. Indeed, as has been recalled in the preceding section, a closed-form solution of the momentum and energy balance equations is available in this special case [12,16]. Also for fully developed laminar mixed convection in a vertical circular duct with a uniform wall heat flux, a closed-form solution of the balance equations, expressed in terms of Bessel functions, is available in the literature [11,19]. As can be easily checked, even in this case, no pre-heating or pre-cooling effects are induced by flow reversal.

The case of free convection, i.e. the case of a purely buoyancy-driven flow, can be investigated by considering  $Gr/Re = (Gr/Re)''$  for a given aspect ratio  $\sigma$ . Obviously, in the case of free convection, the friction factor  $f$  is identically zero, since a purely buoyancy-driven flow is obtained in the limit  $dP/dZ \rightarrow 0$ . The Nusselt number for free convection, evaluated according to the definition expressed by Eq. (25), is denoted through the symbol  $Nu''$ . Values of  $Nu''$  for different aspect ratios are reported in Table 1. These values allow one to conclude that  $Nu''$  strictly increases with  $\sigma$  and reaches a maximum for  $\sigma = 1$ . In Fig. 8, plots of the dimensionless velocity distribution  $u(x, y)$  and of the dimensionless temperature  $t(x, y)$  for the case of free convection are reported for a square duct. On account of Table 1, the condition of free convection in a square duct is reached for

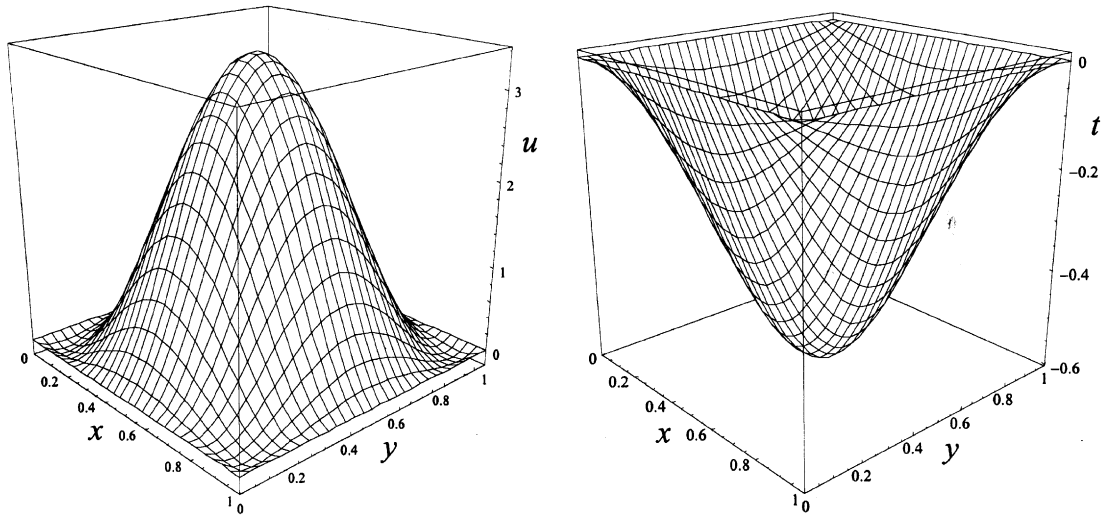


Fig. 8. Plots of  $u(x,y)$  (upper frame) and  $t(x,y)$  (lower frame) for a square duct ( $\sigma = 1$ ) in the case of free convection, i.e. for  $Gr/Re = (Gr/Re)''$ .

$Gr/Re = (Gr/Re)'' = -273.77$ . The plot of  $u(x,y)$  in Fig. 8 shows that a slight flow reversal occurs, while the plot of  $t(x,y)$  shows that there are no points with  $t > 0$ , i.e. there is no pre-heating or pre-cooling effect.

**6. Conclusions**

Fully developed and laminar mixed convection in a rectangular duct has been investigated with reference to an H1 thermal boundary condition, i.e. an axially uniform wall heat flux and a peripherally uniform wall temperature have been assumed. The Boussinesq approximation has been invoked and the reference temperature for the linearization of the equation of state  $\varrho = \varrho(T)$  has been chosen as the mean temperature in a duct cross-section,  $T_0$ . The governing equations have been written in a dimensionless form revealing that both the dimensionless velocity and the dimensionless temperature are two-dimensional fields, so that they can be expressed as  $u(x,y)$  and  $t(x,y)$ . These fields are uniquely determined by a pair of dimensionless parameters, i.e. the ratio  $Gr/Re$  and the aspect ratio  $\sigma$ . The dimensionless governing equations have been solved analytically by employing a finite Fourier transforms method. For a fixed aspect ratio  $\sigma$ , the following relevant features of the solution have been pointed out.

- There exists a negative real number  $(Gr/Re)'$  such that for  $Gr/Re < (Gr/Re)'$  the velocity field displays the phenomenon of flow reversal, i.e. there exist domains within the duct where the dimensionless velocity  $u = U/U_0$  is negative.

- There exists a negative real number  $(Gr/Re)'' < (Gr/Re)'$  such that: the Fanning friction factor  $f$  vanishes for  $Gr/Re = (Gr/Re)''$ ; there exist no zeros of  $f$  for  $0 > Gr/Re > (Gr/Re)''$ . When  $Gr/Re = (Gr/Re)''$  a purely buoyancy-driven flow (free convection) occurs.
- There exists a negative real number  $(Gr/Re)_t$  such that for  $Gr/Re < (Gr/Re)_t$  there are domains within the duct where the dimensionless temperature  $t$  assumes positive values. In other words, for  $Gr/Re < (Gr/Re)_t$  the fluid experiences pre-heating (pre-cooling) effects.
- There exists a negative real number  $(Gr/Re)''' < (Gr/Re)''$  such that: both the dimensionless temperature field  $u(x,y)$  and the dimensionless temperature field  $t(x,y)$  are singular for  $Gr/Re = (Gr/Re)'''$ ; there exist no zeros of the friction factor  $f$  in the open interval  $(Gr/Re)''' < Gr/Re < (Gr/Re)''$ ; there exist no singularities of the distributions  $u(x,y)$  and  $t(x,y)$  for  $(Gr/Re)''' < Gr/Re < 0$ .

Values of  $(Gr/Re)'$ ,  $(Gr/Re)''$ ,  $(Gr/Re)'''$  and  $(Gr/Re)_t$  have been tabulated for different aspect ratios.

The solution obtained in the present paper has been compared with other existing solutions referring to the same heat transfer problem or to special cases. In particular, an interesting comparison with the analytical solution found by Han [3] for the same heat transfer problem has revealed that quite important discrepancies exist in the values of  $f Re$  and of  $Nu$ . These discrepancies are due to the different choice of the reference temperature for the linearization of the equation of state  $\varrho = \varrho(T)$ . Indeed, Han [3] performed the linearization around the wall temperature  $T_w$ .

**References**

- [1] A. Barletta, Analysis of flow reversal for laminar mixed convection in a vertical rectangular duct with one or more isothermal walls, *International Journal of Heat and Mass Transfer* 44 (2001) 3481–3497.
- [2] J.P. Hartnett, M. Kostic, Heat transfer to Newtonian and non-Newtonian fluids in rectangular ducts, *Advances in Heat Transfer* 19 (1989) 247–356.
- [3] L.S. Han, Laminar heat transfer in rectangular channels, *ASME Journal of Heat Transfer* 81 (1959) 121–128.
- [4] D.B. Ingham, D.J. Keen, P.J. Heggs, Flows in vertical channels with asymmetric wall temperatures and including situations where reverse flows occur, *ASME Journal of Heat Transfer* 110 (1988) 910–917.
- [5] C. Gau, K.A. Yih, W. Aung, Reversed flow structure and heat transfer measurements for buoyancy-assisted convection in a heated vertical duct, *ASME Journal of Heat Transfer* 114 (1992) 928–935.
- [6] C.-H. Cheng, C.-J. Weng, W. Aung, Buoyancy effect on the flow reversal of three-dimensional developing flow in a vertical rectangular duct – a parabolic model solution, *ASME Journal of Heat Transfer* 117 (1995) 236–241.
- [7] C.-H. Cheng, S.-Y. Huang, W. Aung, Enhancement of FLARE method for predicting buoyancy-induced flow reversal in vertical ducts via parabolic model, *Numerical Heat Transfer B* 31 (1997) 327–345.
- [8] K.-T. Lee, Laminar natural convection heat and mass transfer in vertical rectangular ducts, *International Journal of Heat and Mass Transfer* 42 (1999) 4523–4534.
- [9] G.D. McBain, Fully developed laminar buoyant flow in vertical cavities and ducts of bounded section, *Journal of Fluid Mechanics* 401 (1999) 365–377.
- [10] C.-H. Cheng, C.-J. Weng, W. Aung, Buoyancy-assisted flow reversal and convective heat transfer in entrance region of a vertical rectangular duct, *International Journal of Heat and Fluid Flow* 21 (2000) 403–411.
- [11] B.R. Morton, Laminar convection in uniformly heated vertical pipes, *Journal of Fluid Mechanics* 8 (1960) 227–240.
- [12] A. Barletta, Heat transfer by fully developed flow and viscous heating in a vertical channel with prescribed wall heat fluxes, *International Journal of Heat and Mass Transfer* 42 (1999) 3873–3885.
- [13] A. Barletta, E. Zanchini, On the choice of the reference temperature for fully-developed mixed convection in a vertical channel, *International Journal of Heat and Mass Transfer* 42 (1999) 3169–3181.
- [14] L. Debnath, *Integral Transforms and Their Applications*, CRC Press, New York, 1995 (Chapter 8).
- [15] M. Spiga, G.L. Morini, A symmetric solution for velocity profile in laminar flow through rectangular ducts, *International Communications in Heat and Mass Transfer* 21 (1994) 469–475.
- [16] Y.-C. Chen, J.N. Chung, The linear stability of mixed convection in a vertical channel flow, *Journal of Fluid Mechanics* 325 (1996) 29–51.
- [17] A. Barletta, Laminar mixed convection with viscous dissipation in a vertical channel, *International Journal of Heat and Mass Transfer* 41 (1998) 3501–3513.
- [18] A. Barletta, Analysis of combined forced and free flow in a vertical channel with viscous dissipation and isothermal–isoflux boundary conditions, *ASME Journal of Heat Transfer* 121 (1999) 349–356.
- [19] A. Barletta, E. Rossi di Schio, Effect of viscous dissipation on mixed convection heat transfer in a vertical tube with uniform wall heat flux, *Heat and Mass Transfer* (in press).